

High resolution (${}^3\text{He},t$) experiment on the double- β decaying nuclei ${}^{128}\text{Te}$ and ${}^{130}\text{Te}$

P. Puppe,¹ A. Lennarz,¹ T. Adachi,² H. Akimune,³ H. Ejiri,^{4,5} D. Frekers,^{1,*} H. Fujita,⁶ Y. Fujita,^{4,6} M. Fujiwara,⁷ E. Ganioglu,⁸ E.-W. Grewe,^{1,†} K. Hatanaka,⁴ R. Hodak,⁹ C. Iwamoto,³ N. T. Khai,¹⁰ A. Okamoto,³ H. Okamura,^{4,‡} P. P. Povinec,⁹ G. Susoy,⁸ T. Suzuki,⁴ A. Tamii,⁴ J. H. Thies,¹ and M. Yosoi¹¹

¹*Institut für Kernphysik, Westfälische Wilhelms-Universität, 48149 Münster, Germany*

²*Research Center for Electron and Photon Science, Tohoku University, Sendai, Miyagi 982-0826, Japan*

³*Department of Physics, Konan University, Kobe 658-8501, Japan*

⁴*Research Center for Nuclear Physics, Osaka University, Ibaraki, Osaka 567-0047, Japan*

⁵*Nuclear Science, Czech Technical University, Prague, Czech Republic*

⁶*Department of Physics, Osaka University, Toyonaka, Osaka 560-0043, Japan*

⁷*Gifu University, Yanagido, Gifu 501-1193, Japan*

⁸*Department of Physics, Science Faculty, Istanbul University, 34134 Vezneciler, Istanbul, Turkey*

⁹*Department of Nuclear Physics and Biophysics, Comenius University, 84248 Bratislava, Slovakia*

¹⁰*Center for Nuclear Science and Technology, Hanoi, Vietnam*

¹¹*Graduate School of Sciences and Technology, Niigata University, Nishi, Niigata 950-2181, Japan*

(Received 5 July 2012; published 1 October 2012)

Gamow-Teller (GT) strength distributions have been investigated in a high-resolution (${}^3\text{He},t$) charge-exchange experiment on the double- β ($\beta\beta$) decaying nuclei ${}^{128}\text{Te}$ and ${}^{130}\text{Te}$. The experiment was carried out at the Research Center for Nuclear Physics, Osaka, with a 420-MeV incident ${}^3\text{He}$ beam and the Grand Raiden magnetic spectrometer. A final-state energy resolution of 35 keV was achieved. The extracted GT strength distributions at low excitation energies in the final nuclei ${}^{128}\text{I}$ and ${}^{130}\text{I}$ are presented and discussed in the context of the $\beta\beta$ decay matrix elements for the two tellurium nuclei. The additional neutron pair in ${}^{130}\text{Te}$ seems to produce a moderate increase in the fragmentation of the low-energy GT distribution.

DOI: [10.1103/PhysRevC.86.044603](https://doi.org/10.1103/PhysRevC.86.044603)

PACS number(s): 25.55.Kr, 21.10.Hw, 23.40.Hc, 27.60.+j

I. INTRODUCTION

The nuclear matrix element for double- β ($\beta\beta$) decay is an essential and highly nontrivial nuclear physics ingredient, which governs the rate of a particular $\beta\beta$ decay. The situation is particularly complex for the neutrinoless decay, since the appearance of a neutrino and its subsequent annihilation at the interaction vertex proceed with a significant exchange of momentum up to ≈ 100 MeV/ c . Model calculations on the basis of the quasi-particle random phase approximation (QRPA), the (interacting) shell model (ISM), the interacting boson model (IBM), or various extensions of these are presently the only means for evaluating these matrix elements [1–4]. In the $2\nu\beta\beta$ decay case, however, the momentum transfer is given by the reaction $Q_{\beta\beta}$ value, and the nuclear matrix element can be constructed from allowed $0^+ \rightarrow 1^+$ Gamow-Teller (GT) transitions in the zero-momentum limit according to

$$(T_{1/2}^{2\nu})^{-1} = G^{2\nu}(Q_{\beta\beta}, Z) |M_{\text{DGT}}^{2\nu}|^2, \quad (1)$$

with the GT $\beta\beta$ decay nuclear matrix element

$$M_{\text{DGT}}^{2\nu} = \sum_m \frac{M_m(\text{GT}^+) \cdot M_m(\text{GT}^-)}{1/2 Q_{\beta\beta} + E_x(1_m^+) - E_0}. \quad (2)$$

Here, $E_x(1_m^+) - E_0$ is the energy difference between the m th intermediate 1^+ state and the initial ground state (g.s.).

$G^{2\nu}(Q_{\beta\beta}, Z)$ is a phase-space factor, and the calculated values for most $\beta\beta$ decaying nuclei are given in, e.g., Ref. [5].

The single β decay matrix elements $M_m(\text{GT}^\pm)$ in Eq. (2) are readily accessible experimentally through intermediate energy charge-exchange reactions of the isospin lowering (p,n) and isospin raising (n,p) type, and the observable strength of a particular GT transition is connected to the matrix element by

$$B_m(\text{GT}^\pm) = |M_m(\text{GT}^\pm)|^2. \quad (3)$$

Charge-exchange studies are therefore an important tool capable of giving insight into the details of the weak nuclear response, which theoretical models dealing with the complex neutrinoless decay need to be confronted with [1–3,5–15]. This has been shown in recent high-resolution (${}^3\text{He},t$) studies on ${}^{76}\text{Ge}$ and ${}^{136}\text{Xe}$ [16,17], where one was led to conclude that the specifics of the nuclear wave functions of the participating nuclei have a significant bearing on the size of the $\beta\beta$ decay matrix elements.

In this article, we focus on the $\beta\beta$ decaying Te isotopes ${}^{128}\text{Te}$ and ${}^{130}\text{Te}$ and present GT distributions obtained from a high-resolution (${}^3\text{He},t$) charge-exchange experiment. The element tellurium is one of the rare cases in the nuclear chart that features two $\beta^-\beta^-$ decaying isotopes side by side, i.e., ${}^{128}\text{Te}$ and ${}^{130}\text{Te}$. The fact that each isotope also exhibits the rather high isotopic abundance of more than 30% makes their decays an interesting geochemical test case. Counting experiments, on the other hand, have focused on ${}^{130}\text{Te}$, because of its higher decay energy, $Q_{\beta\beta} = 2527.51(1)$ keV [18], and thereby larger phase-space factor, compared to the $Q_{\beta\beta} = 866.5(9)$ keV for ${}^{128}\text{Te}$. COBRA [19,20], CUORE [21,22], and NEMO [23]

*frekers@uni-muenster.de

†Present address: RWE Vertrieb AG, Dortmund, Germany.

‡Deceased.

are presently the experiments actively investigating its decay properties.

Tellurium minerals and ore inclusions in ancient and unaltered rock samples gave the earliest evidence for $\beta\beta$ decay through the observation of isotopic anomalies of trapped xenon gas caused by the accumulation of the decay daughters ^{128}Xe and ^{130}Xe . The first measurements of this kind were reported by Inghram and Reynolds [24,25] as early as 1949. These authors even quoted a half-life for ^{130}Te of $T_{1/2} = 1.4 \times 10^{21}$ yr [25], which, given today's knowledge, appears to be too long by a factor of 2. On the other hand, isotopic anomalies of trapped xenon can be generated by a multitude of environmental and cosmogenic reactions including those induced by α particles, neutrons, neutrinos, and muons [26–28]. Takaoka and Ogata [26] provided a first comprehensive and meticulously conducted analysis of mass spectroscopy measurements of trapped xenon isotopes in rock samples from Japan and concluded that the ^{130}Xe anomaly was unambiguously a result of the ^{130}Te $\beta\beta$ decay, whereas the slight enhancement of the ^{128}Xe component was deemed to be only a likely result of the ^{128}Te decay. Kirsten *et al.* [27] reported a value for the ^{130}Te half-life of $T_{1/2} = (6 \pm 3) \times 10^{20}$ yr, which is close to the presently accepted one, but it was revised in Ref. [29] to $T_{1/2} = (2.2 \pm 0.7) \times 10^{21}$ yr.

For many years a discrepancy persisted in the geochemically determined half-lives. There seemed to be a set of short half-life measurements obtained from rather recent tellurium deposits, dating back to about 100 million years [30–33], and a set of long ones obtained from more ancient rock samples, dating back to a billion years [29,34–37]. These results were critically reviewed in Refs. [38] and [39], where the authors suggested that the shorter half-life measurements are more credible. The shorter half-life was also confirmed by a direct counting-rate measurement from the NEMO Collaboration [23]. The recently reported ^{130}Te $2\nu\beta\beta$ decay half-life is $T_{1/2}^{2\nu} = 7.0^{+0.9(\text{stat})}_{\pm 1.1(\text{syst})} \times 10^{20}$ yr [23,40]. Given the geochemically accepted isotopic daughter-nuclei ratio $R(\frac{^{128}\text{Xe}}{^{130}\text{Xe}}) = (3.52 \pm 0.11) \times 10^{-4}$ [41], the half-life of ^{128}Te is evaluated as $T_{1/2}^{2\nu} = (1.9 \pm 0.4) \times 10^{24}$ yr [42]. Considering the calculated phase-space factors from Ref. [5], this leads to a relatively large difference between the two matrix elements in Eq. (2), namely,

$$M_{\text{DGT}}^{2\nu}(^{128}\text{Te}) \approx 1.4 \cdot M_{\text{DGT}}^{2\nu}(^{130}\text{Te}), \quad (4)$$

or, according to Eq. (1), an accelerated decay of ^{128}Te over ^{130}Te by a factor of 2.

The aim of the present charge-exchange experiment is threefold:

- (i) A charge-exchange reaction experiment on ^{130}Te will provide detailed information about the low-lying GT^- strength distribution, for which presently only medium-resolution (p,n) data exist [43]. The GT^- transition strength defines one “leg” of the $2\nu\beta\beta$ decay matrix element, and a high-resolution measurement constrains theoretical models dealing with the ^{130}Te $\beta\beta$, the 2ν and the 0ν decay alike.
- (ii) A comparison of the charge-exchange reactions on ^{128}Te and ^{130}Te will elucidate the role that the additional

neutron pair near the $N = 82$ closed shell may play for $\beta\beta$ decay. From the measurements of the Xe isotopic ratios one would be led to the conclusion that there is a marked effect on the $2\nu\beta\beta$ decay matrix elements.

- (iii) The technique of extracting $B(\text{GT})$ values follows a given standard recipe in the distorted-wave Born approximation (DWBA), which is based on the effective nucleon-nucleon t matrix given by Love and Franey [44,45] and the reaction model of Kerman, McManus, and Thaler [46]. Since the $^{128}\text{I}(1^+) \rightarrow ^{128}\text{Te}(0^+)$ weak decay ft value is known, the hadronic charge-exchange reaction on ^{128}Te is an important anchor point to check the validity of the procedure in the medium to high mass range. This is a fortuitous side effect of the present study.

II. EXPERIMENT

The experiment was performed at the Research Center for Nuclear Physics (RCNP), Osaka University, Japan. A 420-MeV ^3He beam was focused on the target located in the scattering chamber at the entrance of the Grand Raiden magnetic spectrometer. The WS beam line [47] provided the necessary dispersion of the beam for the best resolution [48]. Several tuning techniques for the dispersion matching between beam line and spectrometer were employed to optimize the momentum and angle resolution [49–51].

Various targets were prepared by evaporating $^{\text{nat}}\text{Te}$ and isotopically enriched ^{128}Te and ^{130}Te at 98.17% and 99.48% onto ^{12}C and $^{\text{nat}}\text{C}$ backing foils of $\approx 90\text{--}130 \mu\text{g}/\text{cm}^2$ areal density. Although brittle and difficult to handle, the advantage of the ^{12}C backing is the absence of ^{13}C , which would cause a contamination of the spectra in the low excitation-energy region of ^{128}Te and ^{130}Te . The areal densities of the Te component of the targets were between 1.26 and 1.57 mg/cm^2 . These were determined by energy-loss measurements of α particles from a calibration source containing the three radioisotopes ^{239}Pu , ^{241}Am , and ^{244}Cm , which feature three strong decay branches, at 5.154 MeV (^{239}Pu), 5.486 MeV (^{241}Am), and 5.805 MeV (^{244}Cm). The ratio of the target thicknesses was further confirmed through the use of the $^{\text{nat}}\text{Te}$ target and an analysis of the strongest transitions from ^{128}Te and ^{130}Te . Background measurements were performed with ^{12}C and with the $^{\text{nat}}\text{C}$ backing targets, however, not at all angles and not with similar statistics as for the Te targets. Further, the ^{12}C foils contained some additional contamination, which partly limited its use. This contamination was absent in the $^{\text{nat}}\text{C}$ foils.

The energy calibration of the ($^3\text{He},t$) spectra was performed using the carbon reaction peaks appearing in the spectra, as well as using spectra taken with a magnesium target, which provides several well-known states between about 4 and 17 MeV in the Te excitation frames. The final accuracy achieved for the absolute energy calibration of the Te spectra was about ± 2 keV. Data were taken at two spectrometer-angle settings, i.e., 0° and 2.5° , which allowed the generation of angular distributions ranging from $\approx 0^\circ\text{--}4^\circ$. Off-line aberration corrections were applied to achieve a final energy resolution of 35 keV.

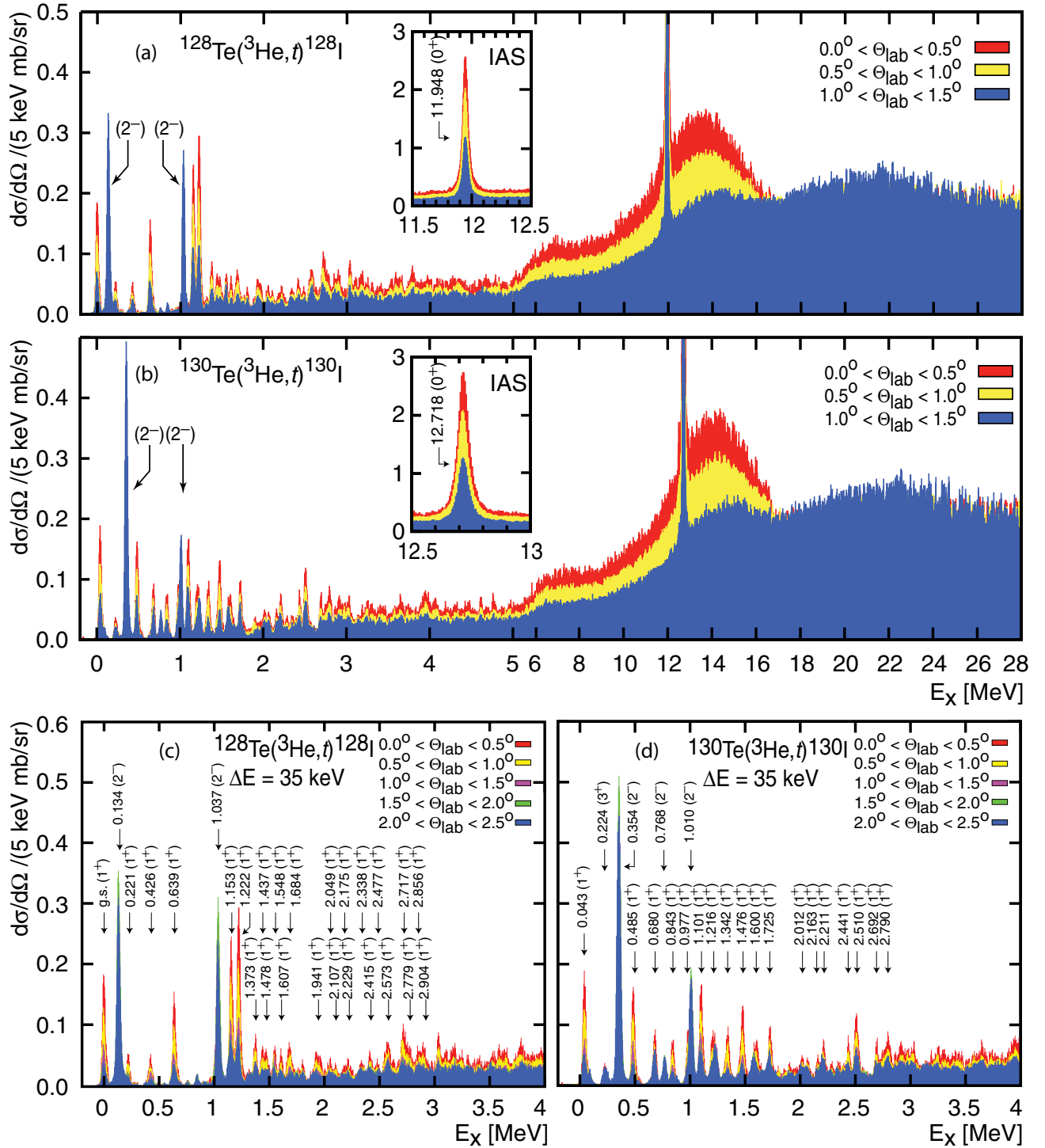


FIG. 1. (Color) Excitation-energy spectra of the (a) ${}^{128}\text{Te}({}^3\text{He}, t){}^{128}\text{I}$ and (b) ${}^{130}\text{Te}({}^3\text{He}, t){}^{130}\text{I}$ reactions. Spectra are generated from several angle cuts (color-coded) and stacked on top of each other to indicate the angular dependence of certain transitions. Forward-peaked transitions are likely of a $\Delta L = 0$ nature, whereas $\Delta L \geq 1$ transitions are more backward-peaked. Insets: Isobaric analog states (IASs) at 11.948 MeV (${}^{128}\text{Te}$) and 12.718 MeV (${}^{130}\text{Te}$). The giant GT resonances appear at $E_x \approx 14$ MeV, and the spin-dipole resonances at $E_x \approx 22$ MeV. Two strong dipole transitions are observed near and below $E_x = 1$ MeV in each reaction. Contaminating carbon transitions have been removed from the spectra. Note the different scales above 5 MeV. (c, d) The low excitation-energy regions shown separately.

III. ANALYSIS

The excitation-energy spectra for the reactions on ${}^{128}\text{Te}$ and ${}^{130}\text{Te}$ at three angles are shown in Fig. 1. The spectra

are stacked on top of each other to indicate their angular dependence, i.e., transitions with $\Delta L = 0$ are typically forward peaked and masked by $\Delta L \geq 1$ transitions. At $E_x = 11.948(2)$

MeV and $E_x = 12.718(2)$ MeV, one observes the isobaric analog states (IASs) of ^{128}Te and ^{130}Te . The excitation-energy values compare well with those extracted from Ref. [52], which are $E_x = 11.950(22)$ MeV and $E_x = 12.735(22)$ MeV, respectively. The giant GT resonances appear at $E_x \approx 14$ MeV, followed by the spin-dipole resonances at $E_x \approx 22$ MeV. There are numerous isolated 1^+ states below 4 MeV. Two strongly excited states below $E_x \approx 1$ MeV appearing in both systems are assigned as $J^\pi = 2^-$, and the state identified at 224 keV in ^{130}I is assigned as $J^\pi = 3^+$ in accordance with the database of the National Nuclear Data Center at Brookhaven [18]. The ^{128}Te and ^{130}Te spectra are qualitatively similar, including the appearance of two strongly excited and almost equally spaced $J^\pi = 2^-$ states below about 1 MeV with almost identical summed strengths.

Angular distributions were generated for most of the identified states. Calculations were carried out in the DWBA formalism using the reaction codes NORMOD [53] and FOLD [54]. Optical model parameters for ^{90}Zr were taken from Ref. [55] and extrapolated to mass $A \sim 130$. The triton optical potential depths were set to 85% of those for ^3He following Refs. [56,57].

The angular distributions for transitions to ^{128}I and ^{130}I are shown in Fig. 2. A sizable $\Delta L = 2$ component had to be included in the DWBA calculations for most of the 1^+ transitions, similar to an observation made in Ref. [17]. The component was added incoherently due to the lack of a viable underlying model for the nucleus. The shapes of the transitions to the known 2^- states, the 3^+ state at 0.224 MeV (^{130}Te), and the IASs at 11.948 (^{128}Te) and 12.718 MeV (^{130}Te) are well described by the DWBA calculations with a single ΔL transfer.

IV. EXTRACTION OF $B(\text{GT})$ STRENGTH

The extraction of the GT strength from the GT part of the cross section follows the recipe given in Refs. [58,59]:

$$\left. \frac{d\sigma^{\text{GT}}}{d\Omega} \right|_{q=0} = \left(\frac{\mu}{\pi\hbar^2} \right)^2 \frac{k_f}{k_i} N_D^{\sigma\tau} |J_{\sigma\tau}|^2 B(\text{GT}), \quad (5)$$

where the functional form of the $q = 0$ extrapolation is given by the zeroth-order Bessel function $|j_0(qR_0)|^2$, with R_0 being the interaction radius $R_0 = 1.25 \cdot A^{1/3}$ (see, e.g., Ref. [58]).

In Ref. [60] a rather precise value for the volume integral of the effective nucleon-nucleon interaction was extracted, $|J_{\sigma\tau}| = 161.5 \pm 3.5$ MeV fm³, however, for a target mass $A = 71$. This value was also adopted for the present mass range $A \approx 130$ for consistency. Further, following Ref. [57], a closed formula based on an eikonal approximation can be employed for the A dependence of the distortion factor, i.e., $N_D^{\sigma\tau} = \exp(1 - 0.895A^{1/3})$, which in the present case matches the value usually calculated as the ratio between the distorted-wave and the plane-wave cross sections,

$$N_D^{\sigma\tau} = \frac{\sigma_{\text{DW}}(q=0)}{\sigma_{\text{PW}}(q=0)}, \quad (6)$$

to within a few percent.

The $B(\text{GT}^-)$ values for the isolated states up to about 3 MeV extracted according to Eq. (5) are listed in Table I for both nuclei, ^{128}Te and ^{130}Te , and are further displayed as histograms together with their running sums in Fig. 3. Integrated $B(\text{GT})$ values from angular distributions taken for energy bins of 500 keV and spread over 35 keV (i.e., the energy resolution) are shown as boxes between 3 and 5 MeV.

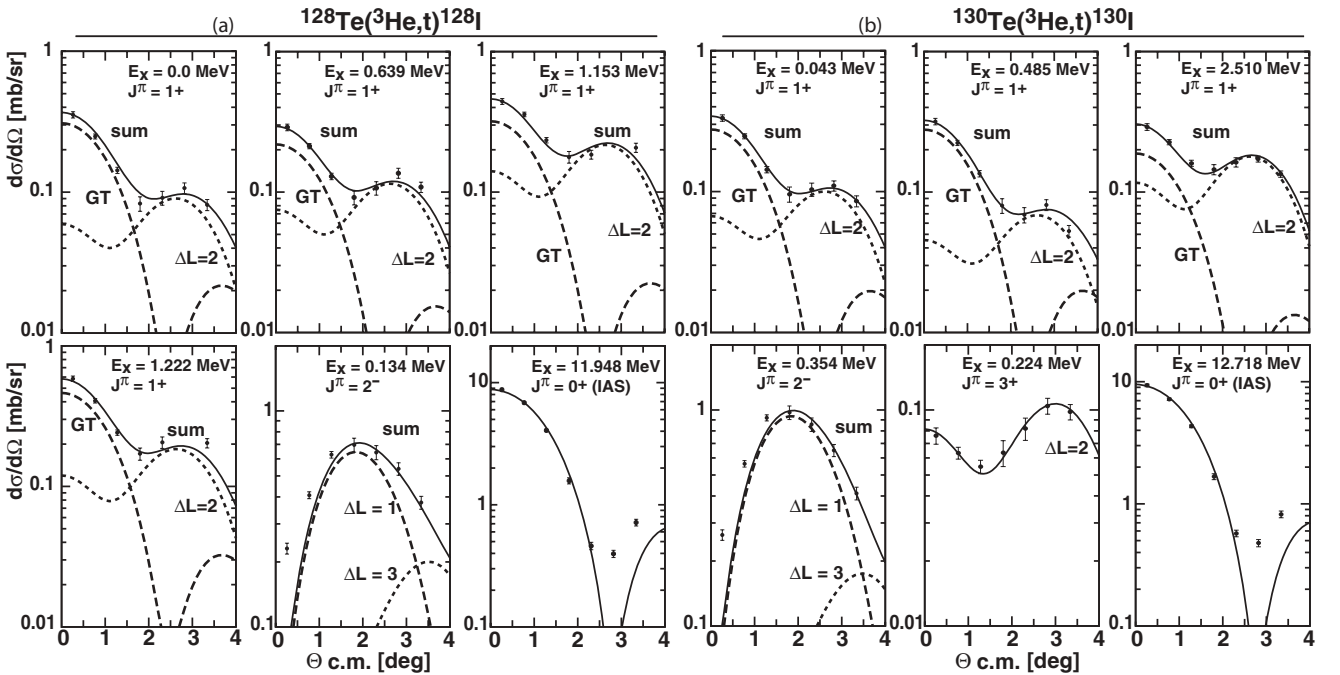


FIG. 2. Angular distributions for several strong transitions of the (a) $^{128}\text{Te}(^3\text{He},t)^{128}\text{I}$ and (b) $^{130}\text{Te}(^3\text{He},t)^{130}\text{I}$ reactions. Some of the 1.153 and 1.222 MeV state data points are omitted because of the difficulty of subtracting the ^{13}C contamination. Error bars denote statistical uncertainties. Solid lines are results of DWBA calculations. Contributing multipolarities are shown as dashed lines.

TABLE I. Energies and spins of states populated in the ${}^{128}\text{Te}({}^3\text{He},t){}^{128}\text{I}$ and the ${}^{130}\text{Te}({}^3\text{He},t){}^{130}\text{I}$ reactions. There are two six-column tables, side by side: one for each isotope. Columns 1 and 2 list excitation energies and spins from Ref. [18]. Excitation energies and spins from the present analysis are given in columns 3 and 4. Excitation energies are determined with an accuracy of ± 2 keV. Spins are deduced from the angular distributions and, in the case of ambiguities, by employing the additional information given in Ref. [18] (as for $J^\pi = 2^-$ or 3^+). Column 5 lists the percentage of the cross section at $q = 0$ attributed to a GT transition using the extraction procedure described in the text. The extracted $B(\text{GT}^-)$ values are listed in column 6.

${}^{128}\text{I}$						${}^{130}\text{I}$					
E_x from Ref. [18] (keV)	J^π	E_x (keV)	J^π	GT (%)	$B(\text{GT}^-)$	E_x from Ref. [18] (keV)	J^π	E_x (keV)	J^π	GT (%)	$B(\text{GT}^-)$
0.0	1^+	0	1^+	84	0.079(8)	43.3	$(1-4)^+$	43	1^+	80	0.072(9)
133.6	2^-	134	2^-	–	–	224.0	3^+	224	3^+	–	–
220.9	$1^+, 2^+, 3^+$	221	1^+	73	0.021(4)	353.7	$(2-5)^-$	354	2^-	–	–
426.3	$1^+, 3^+$	426	1^+	71	0.020(5)			485	1^+	86	0.073(6)
		639	1^+	74	0.057(10)			680	1^+	57	0.027(11)
1036	–	1037	2^-	–	–	768.4	$(2-5)^-$	768	2^-	–	–
		1153	1^+	69	0.084(19)			843	1^+	73	0.027(5)
		1222	1^+	79	0.121(16)			977	1^+	83	0.038(4)
		1373	1^+	52	0.022(11)			1101	1^+	69	0.062(14)
		1437	1^+	63	0.020(6)			1216	1^+	65	0.047(13)
		1478	1^+	58	0.018(7)			1342	1^+	70	0.043(10)
		1548	1^+	65	0.022(6)			1476	1^+	78	0.067(10)
		1607	1^+	40	0.011(8)			1600	1^+	60	0.039(14)
		~ 1684	1^+	71	0.039(8)			1725	1^+	50	0.030(15)
		1941	1^+	65	0.043(13)			2012	1^+	53	0.018(8)
		2049	1^+	50	0.015(8)			2163	1^+	54	0.015(7)
		2107	1^+	47	0.010(6)			2211	1^+	46	0.021(13)
		2175	1^+	53	0.011(5)			2441	1^+	51	0.021(13)
		2229	1^+	56	0.018(8)			2510	1^+	62	0.050(16)
		2338	1^+	47	0.018(11)			2692	1^+	53	0.023(10)
		2415	1^+	46	0.017(10)			2790	1^+	70	0.075(16)
		2477	1^+	46	0.012(8)						$\Sigma = 0.746(45)$
		2573	1^+	59	0.046(17)						
		2717	1^+	65	0.047(13)						
		2779	1^+	52	0.024(12)						
		2856	1^+	54	0.026(12)						
		2904	1^+	60	0.026(10)						
					$\Sigma = 0.829(50)$						

Because of the additional uncertainty with which the non-GT contributions (dotted lines in Fig. 2) are evaluated at $q = 0$, we follow the spirit of Refs. [16,17,60] and assume that 50% of the non-GT part of the cross section at $q = 0$ enters into the error calculation for the GT strength values. Such a conservative error margin then also includes possible non-GT tensor contributions.

A. Impact on $\beta\beta$ decay matrix elements

Clearly, there is no apparent qualitative difference between the $B(\text{GT})$ distributions of the two systems. Even the differences observed in the running sums are small. Since the energy denominators in Eq. (2) for the two Te nuclei are almost identical, the 40% difference in the $\beta\beta$ decay matrix elements, if confirmed, can only originate from differences on the β^+ side. Experimental information about the β^+ side requires, however, (n,p) type charge-exchange experiments on ${}^{128}\text{Xe}$ and ${}^{130}\text{Xe}$.

Yet, upon close inspection of the low-energy excitation region in Fig. 1, one may notice that the g.s. and the 639-keV transitions to ${}^{128}\text{I}$ seem to have mirror partners in ${}^{130}\text{I}$, which are the 43- and 485-keV transitions, similar to the 2^- transition doublet to 134 and 1037 keV (${}^{128}\text{I}$) and to 354 and 1010 keV (${}^{130}\text{I}$). On the other hand, the strong and closely spaced 1^+ doublet at 1153/1222 keV in ${}^{128}\text{I}$ gets fragmented in ${}^{130}\text{I}$ into numerous, almost evenly spaced states as a result of the additional neutron pair in ${}^{130}\text{Te}$. The effect of pairing correlations on the structure of the nuclear matrix elements for Te $\beta\beta$ decay has recently been investigated in Ref. [4] following some earlier experimental and theoretical studies in the mass $A = 76$ system [61–63]. Although the hybrid model advocated in Ref. [4] has some advantages over the standard proton-neutron QRPA, at least as far as the overall size of the matrix elements is concerned, a clear correspondence to the present data situation is not immediately obvious in either of these models.

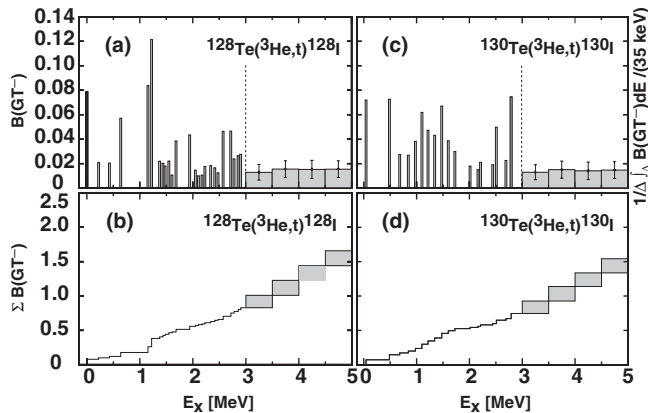


FIG. 3. $B(\text{GT}^-)$ distributions for (a, c) the $^{128,130}\text{Te}(^3\text{He},t)^{128,130}\text{I}$ reactions and (b, d) their running sums. Above 3 MeV the distributions are integrated over ($\Delta = 500$ keV) intervals and distributed into 35-keV bins. Error bars are indicated only for the regions above $E_x = 3$ MeV. For the individual states $E_x \leq 3$ MeV they are reported in Table I.

A rather instructive and intuitive description of the global properties of $2\nu\beta\beta$ decay nuclear matrix elements, e.g., the level of fragmentation in the GT distributions or the occurrence of a single state dominance in certain special cases, is given in Refs. [64,65] in terms of the pairing amplitudes near the relevant proton and neutron Fermi surfaces (Fermi surface quasiparticle model, FSQP). In the FSQP model the single β decay matrix element for the first 1^+ state $M_1(\text{GT}^-)$ is proportional to the product of the neutron occupation and the proton vacancy probabilities ($v_n u_p$). These are comparatively large and nearly equal for ^{128}Te and ^{130}Te , as observed in the present experiment. On the other hand, $M_1(\text{GT}^+)$ is proportional to the product of the proton occupation and neutron vacancy probabilities ($v_p u_n$). These are likely small for the nearly closed neutron-shell Xe isotopes, where u_n is even smaller for ^{130}Xe than for ^{128}Xe , suggesting a significant difference between the two $\beta\beta$ decay matrix elements [65].

Further, the $^{128,130}\text{Te}$ systems fall into the same category as ^{76}Ge , with protons and neutrons near the Fermi surface occupying the same major shell ($N_S = 3$ for ^{76}Ge and $N_S = 4$ for $^{128,130}\text{Te}$). In these cases increased fragmentation of low-lying 1^+ states is expected. From the relative strength of the lowest-lying 1^+ state in each of the systems one can further predict that in the $^{128,130}\text{Te}$ cases the level of fragmentation should be significantly reduced compared to that for ^{76}Ge , which is in remarkable qualitative agreement with the present $(^3\text{He},t)$ data and recent charge-exchange studies on ^{76}Ge and ^{76}Se [16,66]. A quantitative evaluation of the effect of the extra neutron pair in ^{130}Te is, however, still beyond the scope of the model.

B. Comparison with the single β decay matrix element

At this stage it may be instructive to briefly review the experimental technique of extracting GT strength values from the hadronic $(^3\text{He},t)$ reaction at typical intermediate energies. As already indicated, one can use the ft value of the weak $^{128}\text{I}(1^+) \rightarrow ^{128}\text{Te}(0^+)$ electron capture (EC) decay as an anchor

TABLE II. List of parameters as they are extracted or used for the ^{128}Te charge-exchange reaction compared with those evaluated from the EC decay of ^{128}I . Note that the $B(\text{GT})[\text{EC}]$ value already contains the spin factor $(2J_i + 1)$.

Charge-exchange reaction		Weak EC decay	
$B(\text{GT})_{\text{g.s.}}(^3\text{He},t)$	0.079(8)	EC(B.R.)	5.71(40)%
$d\sigma/d\Omega_{\text{g.s.}}^{\text{GT}} _{q=0}$	0.31(3) mb/sr	$\log ft[\text{EC}]$	5.12(3)
N_D	0.0299	$B(\text{GT})[\text{EC}]$	0.087(10)
$ J_{\sigma\tau} $	161.5 MeV fm ³		
$B(\text{F})[\text{IAS}]$	24		
$E_x[\text{IAS}]$	11.948(2) MeV		
$d\sigma/d\Omega_{\text{IAS}}^{q=0}$	11.3(5) mb/sr		
$ J_\tau $	56.5 MeV fm ³		
R^2	8.29(80)		

point. The EC/β^+ branching ratio has been accurately determined by Miyahara *et al.* [67,68] to 5.71(40)%, which leads to a $\log ft = 5.12(3)$ using the National Nuclear Data Center $\log ft$ calculator [18]. These measurements supersede earlier determined branching ratios and $\log ft$ values from Benczer *et al.* [69] and Langhoff *et al.* [70]. Using the most recent value for the axial-vector coupling constant $g_A = 1.2694(28)$ [71], the $B(\text{GT})$ value comes to $B(\text{GT}) = 0.087(10)$, which compares comfortably well with the $B(\text{GT}) = 0.079(8)$ extracted from the present $(^3\text{He},t)$ measurement by using Eq. (5). It also ensures that there are no significant additional mass dependencies between mass $A \approx 70$ and $A \approx 130$ appearing in the effective interaction volume integrals $|J_{\sigma\tau}|^2$ of Eq. (5). A similar situation is found for the Fermi transitions to the IAS, which exhibit the well-known total strength of $B(\text{F}) = (N - Z)$. Taking the extrapolated $q = 0$ cross sections for both Te nuclei and using the same distortion factor N_D as in the GT case, one extracts $|J_\tau| = 56.5$ MeV fm³ for ^{128}Te and $|J_\tau| = 56.6$ MeV fm³ for ^{130}Te , which are almost identical to the value extracted and successfully used in Ref. [60]. Accordingly, the ratio $R^2 = d\sigma_{\text{GT}}^{q=0}/d\sigma_{\text{F}}^{q=0} \cdot B(\text{F})/B(\text{GT})$, also used to evaluate the unit cross section, comes to $R^2 = 8.29(80)$, compared to 8.76(40) for mass $A = 71$ quoted in Ref. [60]. The various extracted quantities for ^{128}Te are listed in Table II for further comparison.

V. CONCLUSION

We performed a high-resolution $(^3\text{He},t)$ charge-exchange experiment at 420 MeV on the $\beta\beta$ decaying nuclei ^{128}Te and ^{130}Te to extract the GT strength distribution in an attempt to further understand the nuclear matrix elements for the $\beta\beta$ decay of the two systems. The GT distributions for the two reactions are found to be qualitatively similar, although the additional neutron pair in ^{130}Te seems to cause some additional fragmentation of states starting at about 1.2 MeV above the ground state. From the presently accepted $\beta\beta$ decay half-lives, one is led to conclude that the decay of ^{128}Te is enhanced by a factor of 2 over that of its neighbor ^{130}Te , because of the larger nuclear matrix element. The present experiment, however, does not exhibit a significant difference between the $B(\text{GT}^-)$ distributions. This is in qualitative agreement with the

FSQP model, which makes the stronger Pauli-blocking effect in ^{130}Te responsible for the difference. An (n,p) type charge-exchange experiment may therefore be required to quantify the effect for these two nuclei.

We have further used the known ft value of the EC decay of ^{128}I as an anchor point to re-evaluate the current methods of extracting $B(\text{GT})$ values from absolute cross-section measurements for medium- to high-mass nuclei and conclude that the $(^3\text{He},t)$ charge-exchange probe does not suffer from any serious unknown mass-dependent effects.

ACKNOWLEDGMENTS

We thank the RCNP accelerator staff for their fine technical support during the course of the experiment. We also thank Y. Yasuda and J. Zenihiro for their effort during the preparation of the experiment. The generous financial support of the RCNP is gratefully acknowledged. Y.F. and A.T. were partly supported by MEXT, Japan, under Grant No. 22540310. The work was partly financed by the Deutsche Forschungsgemeinschaft under Grant No. FR 601/3-1.

-
- [1] V. A. Rodin, A. Faessler, F. Šimkovic, and P. Vogel, *Nucl. Phys. A* **766**, 107 (2006); **793**, 213(E) (2007).
- [2] E. Caurier, J. Menéndez, F. Nowacki, and A. Poves, *Phys. Rev. Lett.* **100**, 052503 (2008).
- [3] J. Barea and F. Iachello, *Phys. Rev. C* **79**, 044301 (2009).
- [4] D. R. Bes and O. Civitarese, *Phys. Rev. C* **81**, 014315 (2010).
- [5] J. Suhonen and O. Civitarese, *Phys. Rep.* **300**, 123 (1998).
- [6] P. Vogel and M. R. Zirnbauer, *Phys. Rev. Lett.* **57**, 3148 (1986).
- [7] A. Staudt, K. Muto, and H. V. Klapdor-Kleingrothaus, *Europhys. Lett.* **13**, 31 (1990).
- [8] E. Caurier, F. Nowacki, A. Poves, and J. Retamosa, *Nucl. Phys. A* **654**, 973c (1999).
- [9] V. A. Rodin, A. Faessler, F. Šimkovic, and P. Vogel, *Phys. Rev. C* **68**, 044302 (2003).
- [10] J. Suhonen, *Phys. Lett. B* **607**, 87 (2005).
- [11] O. Civitarese and J. Suhonen, *Phys. Lett. B* **626**, 80 (2005).
- [12] O. Civitarese and J. Suhonen, *Nucl. Phys. A* **761**, 313 (2005).
- [13] E. Caurier, F. Nowacki, and A. Poves, *Int. J. Mod. Phys. E* **16**, 552 (2007).
- [14] F. Šimkovic, A. Faessler, V. A. Rodin, P. Vogel, and J. Engel, *Phys. Rev. C* **77**, 045503 (2008).
- [15] F. Šimkovic, A. Faessler, H. Mütter, V. Rodin, and M. Stauf, *Phys. Rev. C* **79**, 055501 (2009).
- [16] J. H. Thies, D. Frekers, T. Adachi, M. Dozono, H. Ejiri, H. Fujita, Y. Fujita, M. Fujiwara, E.-W. Grewe, K. Hatanaka *et al.*, *Phys. Rev. C* **86**, 014304 (2012).
- [17] P. Puppe, D. Frekers, T. Adachi, H. Akimune, N. Aoi, B. Bilgier, H. Ejiri, H. Fujita, Y. Fujita, M. Fujiwara *et al.*, *Phys. Rev. C* **84**, 051305 (2011).
- [18] National Nuclear Data Center, Brookhaven National Laboratory (2012); <http://www.nndc.bnl.gov>.
- [19] K. Zuber, *Phys. Lett. B* **519**, 1 (2001).
- [20] K. Zuber, *Prog. Part. Nucl. Phys.* **64**, 267 (2010).
- [21] C. Arnaboldi, F. T. Avignone III, J. Beeman, J. M. Barucci, M. Balata *et al.*, *Nucl. Instrum. Methods Phys. Res. Sec. A* **518**, 775 (2004).
- [22] C. Arnaboldi, D. R. Artusa, F. T. Avignone III, M. Balata, I. Bandac, M. Barucci, J. W. Beeman, F. Bellini, C. Brofferio, C. Bucci *et al.*, *Phys. Rev. C* **78**, 035502 (2008).
- [23] R. Arnold, C. Augier, J. Baker, A. S. Barabash, A. Basharina-Freshville, S. Blondel, M. Bongrand, G. Broudin-Bay, V. Brudanin, A. J. Caffrey *et al.*, *Phys. Rev. Lett.* **107**, 062504 (2011).
- [24] M. G. Inghram and J. H. Reynolds, *Phys. Rev.* **76**, 1265 (1949).
- [25] M. G. Inghram and J. H. Reynolds, *Phys. Rev.* **78**, 822 (1950).
- [26] N. Takaoka and K. Ogata, *J. Mass Spectrom. Soc. Jpn.* **16**, 113 (1968).
- [27] T. Kirsten, W. Gentner, and O. A. Schaeffer, *Z. Phys.* **202**, 271 (1967).
- [28] J. Takagaki, W. Hampel, and T. Kirsten, *Earth Planet. Sci. Lett.* **24**, 141 (1974).
- [29] T. Kirsten, O. A. Schaeffer, E. Norton, and R. W. Stoenner, *Phys. Rev. Lett.* **20**, 1300 (1968).
- [30] E. W. Hennecke, O. K. Manuel, and D. D. Sabu, *Phys. Rev. C* **11**, 1378 (1975).
- [31] J. F. Richardson, O. K. Manuel, B. Sinha, and R. I. Thorpe, *Nucl. Phys. A* **453**, 26 (1986).
- [32] W. J. Lin, O. K. Manuel, G. L. Cumming, D. Krstic, and R. I. Thorpe, *Nucl. Phys. A* **481**, 477 (1988).
- [33] N. Takaoka, Y. Motomura, and K. Nagao, *Phys. Rev. C* **53**, 1557 (1996).
- [34] E. C. Alexander, Jr., B. Srinivasan, and O. K. Manuel, *Earth Planet. Sci. Lett.* **5**, 478 (1968).
- [35] B. Srinivasan, E. C. Alexander, Jr., and O. K. Manuel, *J. Inorg. Nucl. Chem.* **34**, 2381 (1972).
- [36] T. Kirsten, H. Richter, and E. Jessberger, *Phys. Rev. Lett.* **50**, 474 (1983).
- [37] T. Bernatowicz, J. Brannon, R. Brazzle, R. Cowsik, C. Hohenberg, and F. Podosek, *Phys. Rev. Lett.* **69**, 2341 (1992).
- [38] A. P. Meshik, C. M. Hohenberg, O. V. Pravdivtseva, T. J. Bernatowicz, and Y. S. Kapusta, *Nucl. Phys. A* **809**, 275 (2008).
- [39] H. V. Thomas, R. A. D. Patrick, S. A. Crowther, D. J. Blagburn, and J. D. Gilmour, *Phys. Rev. C* **78**, 054606 (2008).
- [40] A. S. Barabash and V. B. Brudanin, *Phys. Atom. Nucl.* **74**, 312 (2011).
- [41] T. Bernatowicz, J. Brannon, R. Brazzle, R. Cowsik, C. Hohenberg, and F. Podosek, *Phys. Rev. C* **47**, 806 (1993).
- [42] A. S. Barabash, *Phys. Rev. C* **81**, 035501 (2010).
- [43] R. Madey, B. S. Flanders, B. D. Anderson, A. R. Baldwin, J. W. Watson, Sam M. Austin, C. C. Foster, H. V. Klapdor, and K. Grotz, *Phys. Rev. C* **40**, 540 (1989).
- [44] W. G. Love and M. A. Franey, *Phys. Rev. C* **24**, 1073 (1981).
- [45] M. A. Franey and W. G. Love, *Phys. Rev. C* **31**, 488 (1985).
- [46] A. K. Kerman, H. McManus, and R. M. Thaler, *Ann. Phys.* **8**, 551 (1959).
- [47] T. Wakasa, K. Hatanaka, Y. Fujita, G. P. A. Berg, H. Fujimura, H. Fujita, M. Itoh, J. Kamiya, T. Kawabata, K. Nagayama *et al.*, *Nucl. Instrum. Methods Phys. Res. Sec. A* **482**, 79 (2002).
- [48] M. Fujiwara, H. Akimune, I. Daito, H. Fujimura, Y. Fujita, K. Hatanaka, H. Ikegami, I. Katayama, K. Nagayama, N. Matsuoka *et al.*, *Nucl. Instrum. Methods Phys. Res. Sec. A* **422**, 484 (1999).
- [49] Y. Fujita, K. Hatanaka, G. P. A. Berg, K. Hosono, N. Matsuoka, S. Morinobu, T. Noro, M. Sato, K. Tamura, and H. Ueno, *Nucl. Instrum. Methods Phys. Res. Sec. B* **126**, 274 (1997).

- [50] H. Fujita, G. P. A. Berg, Y. Fujita, K. Hatanaka, T. Noro, E. J. Stephenson, C. C. Foster, H. Sakaguchi, M. Itoh, T. Taki *et al.*, *Nucl. Instrum. Methods Phys. Res. Sec. A* **469**, 55 (2001).
- [51] H. Fujita, Y. Fujita, G. P. A. Berg, A. D. Bacher, C. C. Foster, K. Hara, K. Hatanaka, T. Kawabata, T. Noro, H. Sakaguchi *et al.*, *Nucl. Instrum. Methods Phys. Res. Sec. A* **484**, 17 (2002).
- [52] F. D. Becchetti, W. S. Gray, J. Jänecke, E. R. Sugarbaker, and R. S. Tickle, *Nucl. Phys. A* **271**, 77 (1976).
- [53] M. A. Hofstee, S. Y. van der Werf, A. M. van den Berg, N. Blasi, J. A. Bordewijk *et al.*, *Nucl. Phys. A* **588**, 729 (1995).
- [54] J. Cook and J. A. Carr, Computer program FOLD, Florida State University, unpublished (1988), based on F. Petrovich and D. Stanley, *Nucl. Phys. A* **275**, 487 (1977), modified as described by J. Cook, K. W. Kemper, P. V. Drumm, L. K. Fifield, M. A. C. Hotchkis, T. R. Ophel, and C. L. Woods, *Phys. Rev. C* **30**, 1538 (1984); R. G. T. Zegers, S. Fracasso, and G. Colò, NSCL, Michigan State University, unpublished (2006).
- [55] J. Kamiya, K. Hatanaka, T. Adachi, K. Fujita, K. Hara, T. Kawabata, T. Noro, H. Sakaguchi, N. Sakamoto, Y. Sakemi *et al.*, *Phys. Rev. C* **67**, 064612 (2003).
- [56] S. Y. van der Werf, S. Brandenburg, P. Grasdijk, W. A. Sterrenburg, M. N. Harakeh *et al.*, *Nucl. Phys. A* **496**, 305 (1989).
- [57] G. Perdikakis, R. G. T. Zegers, Sam M. Austin, D. Bazin, C. Caesar, J. M. Deaven, A. Gade, D. Galaviz, G. F. Grinyer, C. J. Guess *et al.*, *Phys. Rev. C* **83**, 054614 (2011).
- [58] T. N. Taddeucci, C. A. Goulding, T. A. Carey, R. C. Byrd, C. D. Goodman, C. Gaarde, J. Larsen, D. Horen, J. Rapaport, and E. Sugarbaker, *Nucl. Phys. A* **469**, 125 (1987).
- [59] C. D. Goodman, C. A. Goulding, M. B. Greenfield, J. Rapaport, D. E. Bainum, C. C. Foster, W. G. Love, and F. Petrovich, *Phys. Rev. Lett.* **44**, 1755 (1980).
- [60] D. Frekers, H. Ejiri, H. Akimune, T. Adachi, B. Bilgier, B. A. Brown, B. T. Cleveland, H. Fujita, Y. Fujita, M. Fujiwara *et al.*, *Phys. Lett. B* **706**, 134 (2011).
- [61] S. J. Freeman, J. P. Schiffer, A. C. C. Villari, J. A. Clark, C. Deibel, S. Gros, A. Heinz, D. Hirata, C. L. Jiang, B. P. Kay *et al.*, *Phys. Rev. C* **75**, 051301(R) (2007).
- [62] J. Suhonen and O. Civitarese, *Phys. Lett. B* **668**, 277 (2008).
- [63] J. Suhonen and O. Civitarese, *Nucl. Phys. A* **847**, 207 (2010).
- [64] H. Ejiri, *J. Phys. Soc. Jpn.* **78**, 074201 (2009).
- [65] H. Ejiri, *J. Phys. Soc. Jpn.* **81**, 033201 (2012).
- [66] E.-W. Grewe, C. Bäumer, H. Dohmann, D. Frekers, M. N. Harakeh, S. Hollstein, H. Johansson, L. Popescu, S. Rakers, D. Savran *et al.*, *Phys. Rev. C* **78**, 044301 (2008).
- [67] H. Miyahara, H. Matumoto, K. Yanagida, Y. Takenaka, and C. Mori, *Nucl. Instrum. Methods Phys. Res. Sec. A* **336**, 385 (1993).
- [68] H. Miyahara, H. Matumoto, G. Wurdianto, K. Yanagida, Y. Takenaka, A. Yoshida, and C. Mori, *Nucl. Instrum. Methods Phys. Res. Sec. A* **353**, 229 (1994).
- [69] N. Benczer, B. Farrelly, L. Koerts, and C. S. Wu, *Phys. Rev.* **101**, 1027 (1956).
- [70] H. Langhoff, P. Kilian, and A. Flammersfeld, *Z. Phys.* **165**, 393 (1961).
- [71] K. Nakamura *et al.* (Particle Data Group), *J. Phys. G: Nucl. Part. Phys.* **37**, 075021 (2010).